

A Method to Determine Cortical Bone Thickness of Human Femur and Tibia Using Clinical CT Scans

Wenjing Du, Jinhuan Zhang, Jingwen Hu

Abstract Femur and tibia fractures, are commonly seen in motor vehicle crashes. Cortical bone thickness is an important contributor to bone strength and stress-strain distribution in impacts. Current finite-element lower extremity models typically focus on three human sizes (i.e. small female, midsize male, and large male), and do not consider the variation in cortical bone thickness among the whole population. Clinical computed tomography (CT) has been used to determine the cortical bone thickness distribution, but the conventional global thresholding method often fails to offer accurate thickness estimation in thin-cortex areas. In this study, a new local thresholding method was developed to determine cortical bone thickness using clinical CT scans and statistical models of cortical bone thickness for human femur and tibia were also established with respect to sex, age, stature and body mass index (BMI). It was found that the average thickness error of the newly-proposed local thresholding method was less than 0.1 mm. In thin-cortex areas, the proposed method provided more accurate results than the global thresholding method. Statistical analysis suggested that age and BMI significantly affect the cortical bone thickness for both femur and tibia.

Keywords cortical bone thickness, femur, tibia, parametric modelling

I. INTRODUCTION

The increasing use and improvement of occupant restraint systems have reduced fatality and severe injury rates in motor vehicle crashes (MVCs), but the protection of the lower extremity (LE) was not improved as much as that of the head and chest [1]. LE injuries still account for 36% of all AIS2+ injuries sustained by front seat occupants in all frontal crashes [2]. Even though LE injuries are usually not fatal, they can lead to costly rehabilitation and disability, which is a heavy burden for the family and community. Femur and tibia fractures are commonly seen in MVCs and cortical bones are believed to have a dominant effect on bone strength, as they serve as a damage-tolerant structural framework [3]. Aging can cause changes in the shape, size, and cortical thickness of bones and thus lead to increased incidence of bone fractures [4]. Other factors such as stature and body mass index (BMI), can also affect bone morphology [5-9].

Finite element (FE) models are powerful and effective tools to assess human impact responses in MVCs and reproduce bone fractures. Multiple FE femur and tibia models have been developed previously. References [10-12] reported detailed LE models using the geometry extracted from CT and/or magnetic resonance imaging (MRI) data. However, their models could not reflect the variation in cortical bone thickness among the population, and a method to estimate the cortical bone thickness from CT scans was not reported. Reference [8] did a comprehensive job on the development of parametric femur FE models, and the population variation in cortical bone thickness was considered. They used a fixed global thresholding method similar to [13] to segment the cortical bone from clinical CT scans, and the thickness was determined based on the distance between the outer and inner cortical surfaces along the normal direction. However, the estimated cortical thickness values were sensitive to the specified threshold, and may introduce significant errors in thin-cortex areas.

In the field of medical image process, several cortex thickness estimation techniques based on clinical CT scans have been proposed, such as the 50% relative threshold method [14-15]. This method considered bone density, which was usually denoted by HU values in CT images. The threshold was set halfway from the soft tissue HU values to the cortex HU values and from the cortex HU values to the trabecular HU values. It was effective if cortex was thick enough in which case the true cortical bone density equaled to the maximum value of the density profile (expressed in HU values) along a line, but it became unreliable in thin-cortex areas and tended to overestimate cortex thickness. References [16-17] did an extensive research on femoral cortical bone

Wenjing Du is a PhD candidate, and Jinhuan Zhang is a Professor in the State Key Laboratory of Vehicle Safety and Energy at Tsinghua University in Beijing, China. Jingwen Hu is a Research Associate Professor at the University of Michigan Transportation Research Institute, Ann Arbor, MI, USA (phone: +1 734 763 6398, email: jwhu@umich.edu).

thickness measurement from clinical CT data based on the model derived from [14] using a model-fitting method. This technique considered the imaging system’s point spread function (PSF) and required knowledge of the density (expressed in HU values) of the true cortical bone, which was assumed to be a constant value for a given subject. The bone density may vary from location to location, thus assuming the cortical bone density as constant at all measuring vertices/points seemed problematic, and the model-fitting process might not converge. Nevertheless, this was a decent technique of great accuracy. Reference [18-19] then proposed a model-based approach without profile fitting but still shared the assumption of a constant cortex density in [16-17]. Bone material content (BMC, i.e. bone mass) was calculated with three parameters measured in the profile with the help of the 50% relative threshold method. Since there were no model-fitting iterations, computation efficiency was considerably improved.

In this study, a local thresholding method was developed to quantify the thickness in cortex areas of the femur and tibia without model-fitting process or assumption of constant cortex density. Inspired by the 50% relative threshold method, on each local HU value profile, a ratio (not 50%) was employed to define a local threshold that distinguished cortex from soft tissue and trabecular bones. This ratio indicated a relative cortex density compared to the most dense part (where CT value was the highest) without the need to assume a specific cortex density value. Unlike the ‘ground truth’ obtained from high-resolution micro-CT scans in studies [16-17], the proposed method was validated against measurements from a post human mortem human subject (PMHS). Results were compared with the conventional global thresholding method to show validity of this method. FE meshes of a baseline model were morphed and fitted to the geometry surfaces reconstructed from 95 clinical CT scans and the cortical bone thickness at each node was computed using the proposed method. Parametric femur and tibia thickness models were developed to address the effect of sex, age, stature and BMI on cortical bone thickness distribution.

II. METHODS

Several parametric FE models [5-9,20] of different human body parts have been developed using a Radial Basis Function (RBF) based method and the whole process is summarised and illustrated in Fig. 1. These models should include geometry shape and size models and thickness models. However, previous thickness models [8] did not address the cortical bone thickness well. As a key step of the process, the cortical bone thickness can be estimated using the proposed local thresholding method in this study.

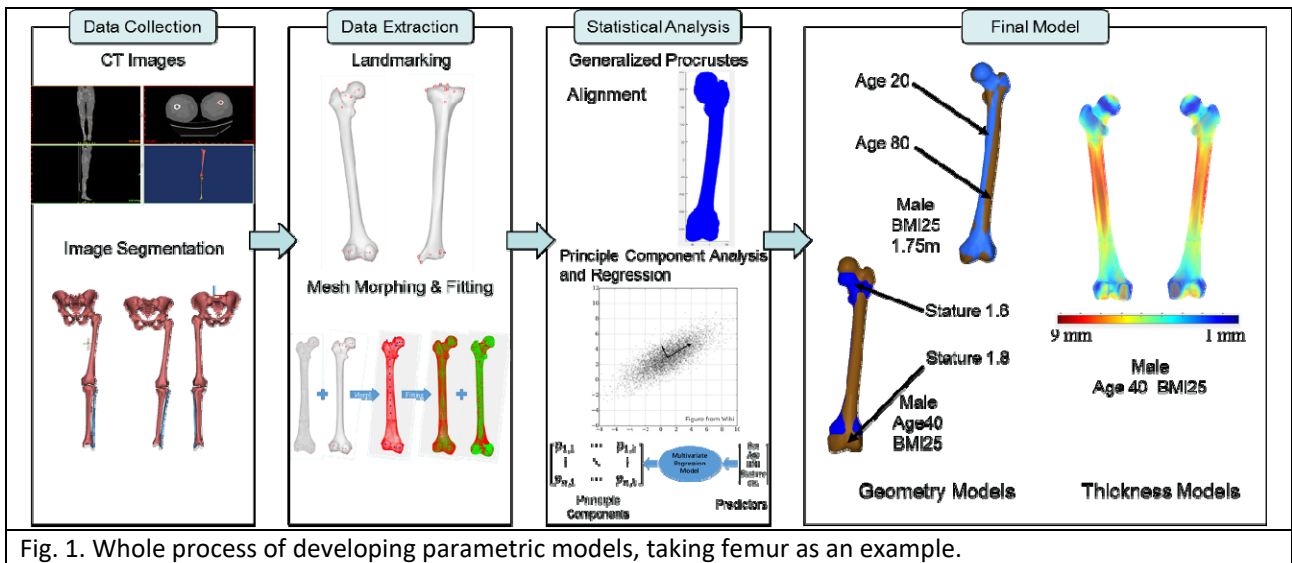


Fig. 1. Whole process of developing parametric models, taking femur as an example.

Bone Geometry Extraction, Morphing and Fitting Techniques

Clinical computed tomography (CT) scans were obtained from multiple hospitals in China through a protocol approved by an institutional review board at Tsinghua University (Beijing, China). All scans in this study were CT angiography scans which covered an entire lower extremity (LE) from pelvis to foot. The CT scans had slice thickness ranging from 0.625 to 1.25 mm with 512×512 pixels on every slice of image. Pixel size varied from

0.623 mm to 1.079 mm. In total, 95 CT scans from 59 male and 36 female patients were collected. Fig. 2 shows that the age range was 16-83 years, and BMI 17.31-32.05 kg/m². No significant correlation between age and BMI was found.

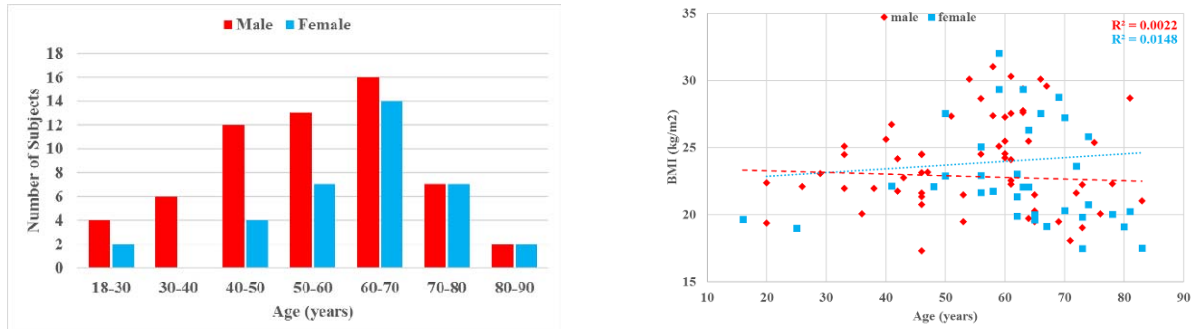


Fig. 2. Subject characteristics distribution.

All CT scans were processed in Mimics (version 19.0, Materialise NV, Belgium). First, a global Hounsfield Unit (HU) threshold value was set to be 210 to segment and reconstruct femurs and tibias in three dimensions, and a series of editing procedures were applied to ensure the bone external surfaces were smooth and water-tight. The bone external surfaces were then exported to Rhinoceros 3D (version 5.0, Robert McNeel & Associates, Seattle, WA) to identify homogenous landmarks on the bone external surfaces of all patients. A total of 23 landmarks at the distal and proximal ends for femur and 16 for tibia were identified. These landmarks were either anatomic landmarks or can be easily distinguished. In the diaphysis region, centroid points of each slice were calculated, which formed the anatomic axes for femur and tibia. This was done by averaging the coordinates of all pixels on each slice whose HU values were above the threshold in Mimics. Eleven points were evenly distributed on the axes and treated as additional landmarks. Instead of putting landmarks on the diaphysis surface, using centroid points can effectively help avoid poor mesh quality in the next few steps.

Femur and tibia meshes from a mid-size male human FE model were used as the template meshes. Following the same protocol mentioned above, homogenous landmarks were also identified on the template mesh. In this study, a landmark-based mesh morphing technique based on a RBF was implemented to morph the template meshes to the bone geometry for each subject. The morphed meshes were then projected to subject geometry surfaces using a customized MATLAB function. It should be noted that the subject geometry surfaces were not necessarily the exterior edge of bone cortex. Nodes on these surfaces offered thickness measuring positions and helped orient the normal direction along which thickness was estimated.

Cortical Bone Thickness Estimation

When the template meshes were morphed and fitted to the geometry of each subject, cortical bone thickness at all the template nodes were calculated. Two methods, global thresholding and local thresholding, were used to estimate the cortical bone thickness as shown in Fig. 3 and Fig. 4. Take femur as an example, a HU value versus point location profile was obtained first for each designated node O' on the subject geometry surface. A 16-millimetre line MN that went through node O' was drawn along the surface normal direction, which was long enough to cover the possible thickest cortex. The start point M of the line was 3 millimetres away outside the template surface. Along the line, 161 evenly-distributed points were sampled with 0.1-millimetre interval. For each sampled point, its HU value was interpolated using a distance-weighted average value of its eight closest voxels with non-zero HU values from CT images according to Equation (1).

$$HU_{est} = \frac{\sum_{i=1}^8 HU_{v,i} \times d_{v,i}}{\sum_{i=1}^8 d_{v,i}} \quad (1)$$

where HU_{est} is the HU value estimated for a given point on MN, $HU_{v,i}$ is the HU value of the i^{th} closest voxel and $d_{v,i}$ is the Euclidean distance from the i^{th} closest voxel to the given point.

The HU value versus point location profile was then smoothed using a thin-plate spline interpolation. Point

location was defined as the Euclidean distance from each sampled point to point M. Without loss of generality, all the profiles were from the bone exterior to the interior.

The global thresholding method used in this study was similar to [8,13]. A fixed HU threshold value, HU_{cor} , was applied to all HU value-location profiles. Values above the threshold were considered cortical bone; while values below the threshold were considered non-cortical bone. The distance between the two points (D and E in Fig. 3) where the HU values were equal or above the threshold was defined as cortical bone thickness.

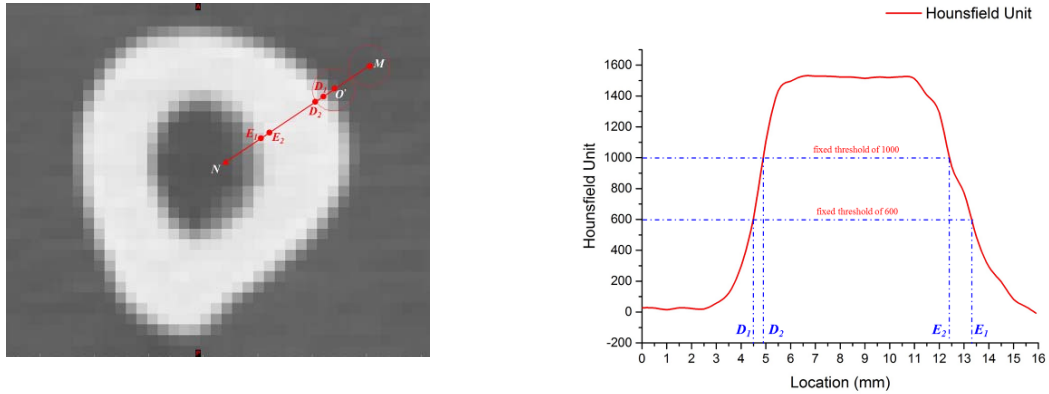


Fig. 3. Cortical bone thickness estimation based on the global thresholding method.

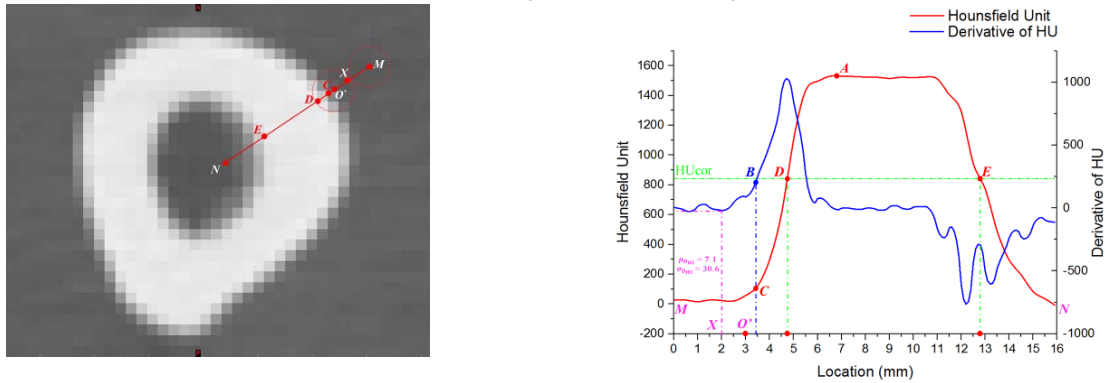


Fig. 4. Cortical bone thickness estimation based on the local thresholding method.

This study proposed a new local thresholding method as illustrated in Fig. 4, in which the HU value threshold for each point was dynamically determined. On the profile, point A was defined as the first maxima point while HU_A was its corresponding HU value. A two-millimetre line MX was defined in the soft tissue area outside the bone structure with relatively low HU values. In the bone area, HU values typically ranged from 200 to 3,000 [21]. The derivative of the HU value-location curve (DHU curve) was calculated, and the DHU from M to X (soft tissue background) should have an average close to zero with a small deviation. To locate a point on DHU whose value was significantly larger than the soft tissue background, a threshold of DHU was defined in Equation (2).

$$DHU_{threshold} = \mu_{DHU} + 4.27\sigma_{DHU} \quad (2)$$

where μ_{DHU} is the mean value of DHU_{MX} , and σ_{DHU} is the corresponding standard deviation. Point B is the first point to reach the threshold $DHU_{threshold}$ on the DHU curve and point C is the corresponding point on the HU curve as point B on the DHU curve. Finally, the cortical bone threshold, $HU_{threshold}$, for this specific HU profile was defined in Equation (3),

$$HU_{threshold} = (HU_A - HU_C) \times K_{cor} + HU_C \quad (3)$$

where HU_A and HU_C are the HU values at points A and C, respectively. K_{cor} is a key coefficient named cortex coefficient that required calibration through experiment.

In this study, cortical bone was identified solely based on HU profiles without any information of cortex bone mineral density (BMD). K_{cor} and the local HU threshold defined a relative density relationship between the cortical bone and the surrounding soft tissue background. We assumed that K_{cor} was a constant in Equation (3), and its value was determined by correlating the estimation to cortical thickness measurements in PMHS, described in the next section.

Cortical Bone Thickness Measurement

The left femur of a PMHS was used to measure cortical bone thickness. The unembalmed PMHS was CT scanned and kept frozen. The femur was put in room temperature to thaw 12 hours prior to the experiment. Five cutting planes were defined in the femur shaft and three more in the femur head, neck and epicondyle, respectively, as shown in Fig. 5a. The cutting was completed following the order from A to H using an electric saw. After each cut, the femur samples were fixed to a clamp on the table and the cross-section was leveled before two photos were taken from the distal and proximal sides with an angle ruler (Fig. 5b and Fig. 6). In addition, a 3D laser scanner was used to obtain the external surface of each cut femur sample. The scanned external surface was translated and rotated to match the CT image based on anatomic landmarks (red round solid dots) as shown in Fig. 5a. At least three non-collinear points on each cutting plane from the external surface were required to define a plane for re-orienting the cross-section from the CT scan. In this way, the cutting planes in the real femur can match the CT images.

Points where cortical bone thickness was measured were marked in the photos and CT images. Vertex normal vectors at all measured points were estimated using a method described in [22]. In the photos, a caliper was used to measure the distance between the measuring point and the boundary where cortical bone and trabecular bone separated. In the femoral head and neck regions, most of the boundaries were distinguishable on the cross section. In the femoral condyle, clear boundaries were not always available and therefore we only recorded the cortical thickness at points where a clear boundary was visible. The distance was then converted to cortical bone thickness in reference to the angle ruler. The cortical bone thickness values at the corresponding points were also calculated using a customised MATLAB code based on the CT images. In this study, 44 points were selected in the photos and CT images. The cortex coefficient K_{cor} was determined through optimisation to minimise the mean squared errors between the calculated thickness values and measured ones. Additionally, 19 more measuring points were selected to cross-validate the coefficient K_{cor} .

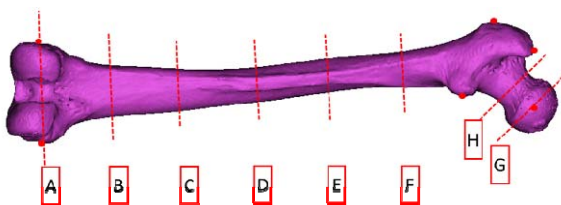


Fig. 5a. Cutting planes in the experiment.

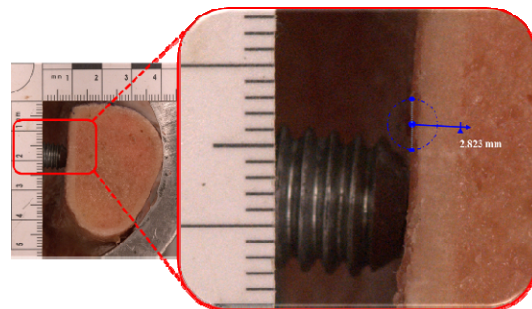


Fig. 5b. Cortical bone thickness measurement.

For a given point P_m , the local threshold corresponding to its HU profile was determined by Equation (3). Assume $K_{cor} = K = 0.001 \times n$, where n was an integer and $n \in (0,1000]$. Let $T_{exp,m,n}$ and $T_{cal,m,n}$ represent thickness measured at the point P_m in the experiment and from the CT scan, respectively. The calculation error at point P_m with $K = 0.001 \times n$ could be denoted as,

$$E_{m,n} = T_{cal,m,n} - T_{exp,m,n} \tag{4}$$

For all possible cortex coefficients K , the mean squared errors between the measured and calculated

thickness values were computed by Equation (5),

$$SS_n = \frac{1}{M} \sum_{m=1}^M E_{m,n}^2 = \frac{1}{M} \sum_{m=1}^M (T_{cal,m,n} - T_{exp,m,n})^2 \quad (5)$$

where SS_n is the mean squared error and $M = 44$, representing the total number of measured points in this study. The K that minimised SS_n would be the cortical coefficient K_{cor} .

Parametric Femur and Tibia Thickness Models

Principal Component Analysis was performed to find out fewer, but sufficient variables called principal components (PCs) that best explained the variance in the original thickness data set using a built-in MATLAB function. All the principal components were orthogonal to each other and formed a new basis to describe the original data in reduced dimensions. A regression analysis was then performed on the PCs with respect to age, BMI and stature and thus parametric femur and tibia thickness models could be developed.

III. RESULTS

Cortical Bone Thickness Measurement

Fig. 6 shows that the corresponding cutting cross-sections in the experiment and the CT image matched well. For each cross section, a point was marked and measured on the most anterior, posterior, medial and lateral edge. Twelve more points and 19 additional validation points were put where necessary and easily distinguishable. All measuring points and validation points were carefully checked to make sure that they were at the same location in the photos as in the CT slices. Three repeated measurements were performed at each measuring point using a caliper. Table I lists some of the thickness results in different femur regions. The percentage errors are shown in the parentheses.

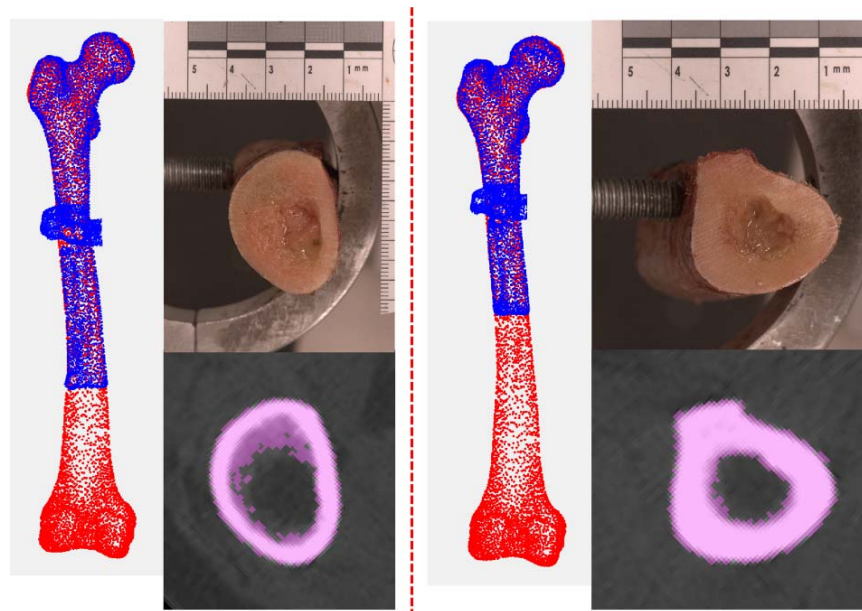


Fig. 6. Femur cutting cross section in the experiment and the CT image. Left: cross section C; Right: cross section D. Blue dots: from the experiment; Red dots: from the CT image.

Cortical Bone Thickness Calculation

For the global thresholding method, the HU threshold was set from 300 to 1,000 with an interval of 100. The mean squared errors between the calculated thickness values and measured ones were also calculated for each HU threshold value.

For the local thresholding method, the cortex coefficient K_{cor} was 0.605 if all 44 measuring points were included and the minimised mean squared error was 0.615 mm². The average estimated thickness based on CT

was 4.26 mm, while the average measured thickness was 4.231 mm. The average thickness error was 0.029 mm (0.685%) and the mean squared error in the validation was 0.626 mm². However, the calculation results showed an underestimation in the femur diaphysis where cortex was thick and an overestimation in the femur epiphysis where cortex was thin. It could also be derived from Equation (3) that a larger K_{cor} would lead to a larger $HU_{threshold}$, which could contribute to the underestimation of thickness in the femur diaphysis. We then proposed to specify two cortex coefficients, 0.860 and 0.522, for thin-cortex and thick-cortex areas, respectively. These cortex coefficients were optimised separately. At this time, the mean squared error reduced to 0.114 mm². The average thickness was 4.214 mm from calculation against 4.231 mm from experiment. The average thickness error dropped to 0.017 mm (0.4%) and the mean squared error in the validation was reduced to 0.044 mm². These results suggested that K_{cor} for femur and tibia shafts was 0.522 and 0.860 for femur and tibia ends. Partial results of both calculation methods are listed in Table I.

TABLE I
CORTICAL BONE THICKNESS (IN MILLIMETERS)

Femur Region	Measured Value	Local Thresholding Method, K_{cor}		Global Thresholding Method				
		0.605	0.860 0.522	400	600	700	800	1000
epiphysis (head)	0.976±0.017	2.1(115.2%)	0.8(-18.0%)	2.9	0.6	0	0	0
	0.960±0.025	1.2(25.0%)	0.9(-6.25%)	0	0	0	0	0
	1.516±0.025	2.7(78.1%)	1.1(-27.4%)	2.1	0	0	0	0
epiphysis (neck)	1.063±0.028	3.6(238.7%)	1.6(50.5%)	2.4	0	0	0	0
	2.196±0.024	2.3(4.7%)	2.7(22.9%)	4.3	2.6	2.1	1.8	0.7
	1.362±0.035	2.1(54.2%)	1.4(2.8%)	2.5	1.9	1.5	0.4	0
	1.121±0.006	1.8(60.6%)	1.1(-1.9%)	2.8	2	1.6	1.3	0
	2.877±0.007	2.8(-2.7%)	3.1(7.8%)	4.5	3.5	3.2	2.9	2.4
diaphysis (shaft)	3.678±0.021	3.6(-2.1%)	3.9(6.0%)	6.3	5.1	4.7	4.2	3.5
	6.749±0.006	6.3(-6.7%)	6.5(-3.7%)	7.7	6.9	6.7	6.5	6.1
	8.700±0.019	8.4(-3.4%)	9.2(5.7%)	13.0	10.3	9.7	9.1	7.4
	6.655±0.034	5.7(-14.4%)	6.4(-3.8%)	8.5	7.0	6.4	5.8	2.5
	4.103±0.021	3.5(-14.7%)	3.9(-4.9%)	5.2	4.6	4.3	3.9	3.4
epiphysis (condyle)	7.946±0.026	7.4(-6.9%)	7.8(-1.8%)	8.9	8.5	8.1	7.8	7.1
	1.178±0.023	2.0(69.8%)	1.0(-15.1%)	2.5	1.3	0.8	0	0
	1.323±0.018	1.4(5.8%)	0.7(-47.1%)	1.2	0	0	0	0
	1.412±0.010	2.1(48.7%)	1.3(-7.9%)	2.8	2.1	1.6	1.3	0

Parametric Femur and Tibia Thickness Models

In this study, parametric thickness models were established for femur and tibia, respectively. Fifty-six PCs were selected for the male femur model and 34 for the female model. The selected PCs were able to account for 99% of all the variance in each model. The coefficient of determination R-squared values were computed for each parametric model using Equation (6),

$$R^2 = 1 - \frac{RSS}{TSS} \tag{6}$$

where RSS is the sum of squared errors between the observed and predicted thickness values, and TSS is the sum of squared differences between the average and observed thickness values. The R-squared values were 0.241 and 0.317 for the male and female femur thickness models, respectively. The R-squared values were

0.186 and 0.301 for the male and female tibia thickness models, respectively. The p-values of the predictors on the first five PCs for each regression model were summarised in Table II. The regression results showed that age and BMI were significant predictors for the femur thickness models while age was the only significant characteristic for the tibia thickness models. Stature was excluded in the predictors because it did not show significant effect on cortical bone thickness distribution.

TABLE II
P-VALUES OF PREDICTORS IN THE THICKNESS MODELS (* p<0.05)

Model	Predictor	p-value				
		1st PC	2nd PC	3rd PC	4th PC	5th PC
Male femur	Age	0.048*	0.000*	0.497	0.430	0.534
	BMI	0.009*	0.916	0.070	0.105	0.089
Female femur	Age	0.203	0.008*	0.006*	0.710	0.555
	BMI	0.291	0.021*	0.878	0.152	0.235
Male tibia	Age	0.035*	0.657	0.002*	0.003*	0.614
	BMI	0.292	0.296	0.287	0.357	0.519
Female tibia	Age	0.001*	0.444	0.048*	0.293	0.311
	BMI	0.130	0.719	0.149	0.820	0.515

IV. DISCUSSION

BMD is the determining factor that distinguishes cortical bone and trabecular bone, and the HU value in CT scans is positively correlated to BMD. Since bones are not made of homogeneous materials, cortical bones in different body areas may sustain different BMDs and thus HUs. Studies [13,14,16] indicate that HU_A (maximum value of the HU profile) may drop considerably in thin-cortex areas because of the resolution limits and blurring effect. Therefore, thresholds that separate cortical and trabecular bone are supposed to vary with local BMDs/HUs in different areas. Conventional global thresholding method fails to consider such local effects. The 50% relative threshold method is robust and effective when cortex is thick enough. However, if the cortex is thin, a fixed ratio of 0.5 may overestimate the cortical thickness. The newly-proposed local thresholding method determines the thresholds based on the local background and maximum HUs, in which case the density variances are considered. The ratio is derived based on a PMHS experiment independent of model assumption. In this study, two different ratios were determined for thin and thick cortex regions, respectively. which can overcome the limitations of the 50% relative threshold method. Since the profile of HU values distribution is obtained in this method independent of pixel sizes, a cortex thickness value can be estimated even if it is thinner than or close to the size of one pixel as shown in Fig. 7.

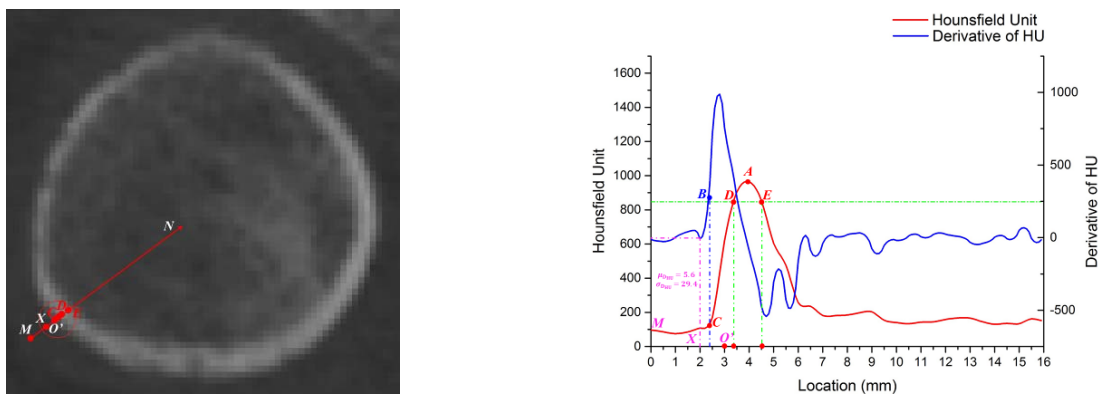


Figure. 7 The local thresholding method in thin-cortex area (femoral neck, pixel size = 0.9766 mm).

In [18], accuracy levels of the 50% relative threshold method, the model-fitting deconvolution method [16-17] and the model-based profile analysis method [18-19] were reported and compared using the standard European Forearm Phantoms. When the true thickness was 1 mm, the smallest percentage error using these three methods was 152.2%, 19.3% and 22.8%, respectively. The error decreased to 18.9%, 0.3% and -0.3%,

respectively when the true thickness became 2 mm. It should be noted that these error levels were from the best estimations under specific scanning conditions which usually could not be met in the clinical CT scanning process. Generally speaking, the local thresholding method proposed in this study is more accurate than the global thresholding method and the 50% relative threshold method in the literature. It may not be as accurate as the model based methods in [16-19], but is still at an acceptable level. However, the accuracy of methods in references [16-19] was quite sensitive to the assumed cortex BMD. An 20% increase of the assumed cortex BMD could lead to an increase of estimation error from +4.3% to -13.1% under the same condition [18]. In contrast, the local thresholding method was more robust as no assumed cortex BMD was needed.

The complex model-based methods mainly focus on the measurement of bone material density or disease diagnosis, such as osteoporosis. The regions of interest are small local areas where fractures are prone to happen. In this study, we focused more on the FE modeling to provide better computational human body models, thus the entire bone is of great concern. Due to radiation dose restriction, resolution of clinical CTs of the entire bone is inferior. Compared the image pixel sizes in this study (0.623 to 1.079 mm) to that mentioned in [16] (0.589 mm), the model-based techniques may not be robust in low resolution clinical CTs. Time efficiency is also important when it comes to modeling. It took a desktop PC around 5 min to process thickness values for 17,000 locations on the femoral neck alone in [16] but less than 1 min to process 9,140 locations on the entire femur in this study. Therefore, even if some complex model-based methods can estimate cortex thickness in sub-millimetre level if condition permits, the local thresholding method proposed in this study that can efficiently estimate thickness results at an acceptable accuracy level still has great potentials in the field.

In this study, two different cortical coefficients were recommended for thin-cortex and thick-cortex areas. In thin-cortex areas, the gap between HU_A and HU_C was smaller than that in thick-cortex areas, but HU_C was similar in all areas. This presented a dilemma, in which a lower K_{cor} was expected for HU profiles in thick-cortex areas but this might overestimate the thickness in thin-cortex areas and vice versa. In order to resolve this issue, thin-cortex and thick-cortex areas were studied separately. Reference [22] used the similar local thresholding method to quantify the cortical bone thickness for human ribs. The average measurement thickness value from the PMHS was 0.796 mm indicating cortex in human ribs was very thin. The cortex coefficient was 0.808 in their study which is close to the value of 0.860 in this study. In thick-cortex areas, a recommended threshold to accurately segment the bone geometry was 49% of the difference of the density between the adjacent tissues [13]. This percentage could be treated as the cortex coefficient K_{cor} , which was again close to the value of 0.522 in this study.

Even though in the thin-cortex areas, the global thresholding method was not reliable, it could still provide acceptable results in the bone shaft areas with a properly selected threshold value. Following the optimisation procedure in this paper, the threshold value can be set to 770. The mean squared error is 0.154 mm² compared to 0.112 mm² using the local thresholding method in the femur shaft area (cross sections B to F). One of the major deficiencies of the global thresholding method is that it cannot guarantee non-zero thickness values at all nodes/points in the model. If this happens, an arbitrary value is usually specified which can introduce obvious errors.

The femur and tibia thickness models did not have high R-squared values. It indicated that the variances in femur and tibia cortical thickness are not well accounted by the current predictors. Therefore, more subject characteristics should be included as predictors in the regression model to increase the correlation. Bone-related diseases, such as osteoporosis and eating habits, may have significant effects on cortical bone thickness distribution. This study indicated that BMI played a significant role in the femur cortical thickness distribution which agreed with the conclusion in [8]. Age was also found to be a significant factor in this study which is not surprising. In [23], it was concluded that the cortical thickness reduced as age advanced for women while cortical thickness was similar at all ages for men. Cortex generally becomes thinner as healthy adults age due to the expansion of marrow area [24]. No results of tibia regression models were given in [8], but this study indicated that BMI was not a significant predictor in tibia cortical thickness.

Several limitations existed in this study. First, only one PMHS was used to calibrate and validate the cortex coefficient. More PMHS will be needed to calibrate the cortex coefficient and validate the proposed method on a larger scale. The sample size of female subjects was small, and no female subjects aged from 30 to 40 were included in this study. Future work will include adding more female clinical CTs to the data set. However, the current sample is at the same level as the previous study (62 male subjects and 36 female subjects in [8]). In the

future, the established parametric external geometry models and thickness models can be integrated as part of the parametric whole-body human body model. Future work may also include extending the proposed method to other body regions.

V. CONCLUSIONS

This study proposed a new local thresholding method to accurately and efficiently estimate cortical bone thickness using clinical CT scans and a method to validate the thickness calculation against experimental results. This study also developed a parametric cortical thickness model accounting for sex, age, stature and BMI effects for human femur and tibia. The models developed in this study can serve as a statistical basis for building parametric FE human models representing a diverse population.

VI. ACKNOWLEDGEMENT

The authors would like to thank Anne Bonifas and Nichole Orton at the University of Michigan Transportation Research Institute in the US for their great help and support in the experiment of femur cortical bone thickness measurement. The authors would also like to thank China Scholarship Counsel for their financial support for this study.

VII. REFERENCES

- [1] Moran S G, McGwin G Jr, Metzger J S, Alonso J E, Rue L W 3rd. Relationship between age and lower extremity fractures in frontal motor vehicle collisions. *The Journal of Trauma*, 2003, 54(2):261-265.
- [2] Kuppaa, S, Fessahaie, O. An overview of knee-thigh-hip injuries in frontal crashes in the United States. *Proceedings of the 18th International Technical Conference on the Enhanced Safety of Vehicles*, 2003, Nagoya, Japan.
- [3] Zimmermann, E A, Busse, B, Gludovatz, B, Ritchie, R O. On the strength and toughness of human cortical bone. *14th International Conference on Fracture*, 2017, Rhodes, Greece.
- [4] Zioupos P, Currey J D. Changes in the stiffness, strength, and toughness of human cortical bone with age. *Bone*, 1998, 22(1):57-66.
- [5] Shi X, Cao L, Reed M P, Rupp J D, Hu J. Effects of obesity on occupant responses in frontal crashes: a simulation analysis using human body models. *Computer Methods in Biomechanics and Biomedical Engineering*, 2015, 18(12):1280-1292.
- [6] Wang Y, Cao L, Bai Z, Reed M P, Rupp J D, Hoff C N, Hu J. A parametric ribcage geometry model accounting for variations among the adult population. *Journal of Biomechanics*, 2016, 49(13):2791-2798.
- [7] Shi X, Cao L, Reed M P, Rupp J D, Hoff C N, Hu J. A statistical human rib cage geometry model accounting for variations by age, sex, stature and body mass index. *Journal of Biomechanics*, 2014, 47(10):2277-2285.
- [8] Klein K F, Hu J, Reed M P, Hoff C N, Rupp J D. Development and validation of statistical models of femur geometry for use with parametric finite element models. *Annals of Biomedical Engineering*, 2015, 43(10):2503-2514.
- [9] Hu, J, Fanta, A, Neal, M O, Reed, M P, Wang, J. Vehicle crash simulations with morphed GHBMC human models of different stature, BMI, and age. *Proceedings of 4th International Digital Human Modeling Conference*, 2016, Montreal, Canada.
- [10] Untaroiu C D, Yue N, Shin J. A finite element model of the lower limb for simulating automotive impacts. *Annals of Biomedical Engineering*, 2013, 41(3):513-526.
- [11] Takahashi, Y, Kikuchi, Y, Mori, F, Konosu, A. Advanced FE lower limb model for pedestrians. *Proceedings of the 18th International Technical Conference on the Enhanced Safety of Vehicles*, 2003, Nagoya, Japan.
- [12] Iwamoto, M, Tamura, A, et al. Development of a finite element model of the human lower extremity for analyses of automotive crash injuries. *SAE Technical Paper*, 2000, Detroit, Michigan, USA.
- [13] Hangartner T N. Thresholding technique for accurate analysis of density and geometry in QCT, pQCT and uCT images. *Journal of Musculoskeletal Neuronal Interact*, 2007, 7(1):9-16.
- [14] Prevrhal S, Engelke K, Kalender W A. Accuracy limits for the determination of cortical width and density: the influence of object size and CT imaging parameters. *Physics in Medicine & Biology*, 1999, 44(3):751-764.
- [15] Prevrhal S, Fox J C, Shepherd J A, Genant H K. Accuracy of CT-based thickness measurement of thin structures: Modeling of limited spatial resolution in all three dimensions. *Medical Physics*, 2003, 30(1):1-8.

- [16]Treece G M, Gee A H, Mayhew P M, Poole K E S. High resolution cortical bone thickness measurement from clinical CT data. *Medical Image Analysis*, 2010, 14(3):276-290.
- [17]Treece G M, Poole K E S, Gee A H. Imaging the femoral cortex: Thickness, density and mass from clinical CT. *Medical Image Analysis*, 2012, 16(5-4):952-965.
- [18]Museyko, O, Gerner, B, Engelke, K. Cortical bone thickness estimation in CT images: A model-based approach without profile fitting. *Third International Workshop and Challenge, Proceedings*, 2015, Munich, Germany.
- [19]Museyko O, Gerner B, Engelke, K. A new method to determine cortical bone thickness in CT images using a hybrid approach of parametric profile representation and local adaptive thresholds: Accuracy results. *PLoS One*, 2017, 12(11): e0187097.
- [20]Li Z, Hu J, et al. Development, validation, and application of a parametric pediatric head finite element model for impact simulations. *Annals of Biomedical Engineering*, 2011, 39(12):2984-2997.
- [21]Schreiber J J, Anderson P A, Rosas H G, Buchholz A L, Au A G. Hounsfield units for assessing bone mineral density and strength: a tool for osteoporosis management. *The Journal of Bone and Joint Surgery, American Volume*, 2011,93(11):1057-1063.
- [22]Li P, Xu S, Du W, Li H, Zhang J. Measurement and characterization of the cortical bone thickness in Chinese human ribs. *Journal of Tsinghua University (Science and Technology)*, 2017, 57(8):815-820.
- [23]Russo C R, Lauretani F, et al. Structural adaptations to bone loss in aging men and women. *Bone*, 2006, 38(1):112-118.
- [24]Clarke B. Normal bone anatomy and physiology. *Clinical Journal of the American Society of Nephrology*, 2008, 3(Suppl 3): S131-S139.